Correlation-Based Super-Resolution Imaging in Microscopy and Ultrasound

Or Dicker, Oren Solomon — Electrical Engineering Department, Technion, Israel — dicker@campus.technion.ac.il, orensol@tx.technion.ac.il

Maor Mutzafi — Physics Department and Solid State Institute, Technion, Israel — maormutz@tx.technion.ac.il

Avinoam Bar-Zion — Biomedical Department, Technion, Israel — barz@tx.technion.ac.il

Mordechai Segev — Physics Department and Solid State Institute, Technion, Israel — msegev@tx.technion.ac.il

Yonina C. Eldar — Electrical Engineering Department, Technion, Israel — yonina@ee.technion.ac.il

***Abstract*—In this work, we demonstrate super-resolution in two traditionally diffraction limited imaging modalities: fluorescence microscopy and contrast enhanced ultrasound imaging. In both cases we exploit the statistical structure of blinking emitters over time, along side their sparse distribution within the imaged object. Our method enables sub-diffraction resolution with high temporal resolution, dictated by the imaging rate of the camera and ultrasound probe, respectively.**

I. Introduction

Traditionally, spatial resolution in imaging is limited by diffraction. Such fundamental limit is present in a variety of imaging modalities. In optical microscopes, spatial resolution is proportional to half of the imaging wavelength, while in ultrasound scans the axial and lateral resolutions are proportional to the wavelength of the transmitted pulse and transducer aperture, respectively. Sub-diffraction imaging techniques such as PALM [1] and STORM [2] alter the measurement process to recover seemingly lost frequencies and achieve unprecedented sub-diffraction resolution. Recently, such methods have also been applied to contrast enhanced ultrasound scans (CEUS) [3], [4] to achieve unprecedented spatial resolution of sub-diffraction vascular structures, in which gas micro-bubbles effectively act as point emitters. However, such methods require many activation cycles and suffer from poor temporal resolution. Another technique, SOFI [5], relies on the temporal statistics of blinking emitters to achieve sub-diffraction resolution with increased temporal resolution. Nonetheless, the spatial resolution of SOFI is fundamentally much lower than that of super-localization methods.

Inspired by SOFI, we propose a framework for achieving super-resolution imaging with temporal resolution comparable to SOFI and spatial resolution comparable to PALM/STORM, which we call sparsity-based super-resolution correlation microscopy (SPARCOM). We exploit the sparse distribution of blinking emitters in the correlation domain, and considerably enhance the spatial resolution of a low resolution movie. We show that SPARCOM recovers super-resolved images with 64-times more pixels than the size of the original low-resolution movie frames by considering its formulation in the discrete Fourier domain. By using a modified gradient-descent algorithm, our formulation leads to a special structure of the gradient which can be computed very efficiently using fast Fourier transform operations.

Inspired by recent work [6], we have also applied similar sparsity based concepts of SOFI to contrast enhanced ultrasound scans in a method we call sparsity-based ultrasound super-resolution hemodynamic imaging (SUSHI), achieving sub-diffraction resolution with a temporal resolution of less than a second.

II. Reconstruction

In microscopy, the imaging system is modeled as a linear space invariant system with a point spread function (PSF) $u(\cdot)$. The acquired fluorescence signal is modeled as a set of L independently fluctuating point sources with resulting fluorescence source distribution

$$f(\mathbf{r},t)=\sum_{k=0}^{L-1}u(\mathbf{r}-\mathbf{r}_k)s_k(t). \tag{1}$$

Each source (or emitter) has its own time dependent brightness function $s_k(t)$, and is located at position $\mathbf{r}_k\in\mathbb{R}^2,\ k=0,\ldots,L-1$.

To increase resolution by exploiting sparsity, we start by introducing a Cartesian sampling grid with spacing Δ_L, which we refer to as the *low-resolution grid*. The low-resolution signal (1) can be expressed over this grid as

$$f[m,n,t]=\sum_{i,j=0}^{N-1}u[mP-i,nP-j]s_{ij}(t),\ m,n=[0,\ldots,M-1]. \tag{2}$$

In (2), we have discretized the possible locations of the emitters $\mathbf{r}_k$, over a discrete Cartesian grid $i,j=0,\ldots,N-1$, $L\ll N$ with resolution Δ_H, such that $[m_k,n_k]=[i_k,j_k]\Delta_H$ for some integers $i_k,j_k\in[0,\ldots,N-1]$. We refer to this grid as the *high-resolution grid*. For simplicity we assume that $\Delta_L=P\Delta_H$ for some $P\geq 1$, and consequently $N=PM$.

Rewriting 2 in vector-matrix notations yields $\mathbf{y}(t)=\mathbf{H}(\mathbf{F}_M\otimes\mathbf{F}_M)\mathbf{s}(t)=\mathbf{A}\mathbf{s}(t)$ with $\mathbf{A}\in\mathbb{C}^{M^2\times N^2}$, where $\mathbf{H}$ is a diagonal matrix whose diagonal corresponds to the low-resolution sampled PSF and $\mathbf{F}_M$ is a partial $M\times N$ discrete Fourier matrix. Denoting the pixel-wise vectorization of $f[m,n,t]$ as $\mathbf{y}(t)$, its correlation matrix is then given by $\mathbf{R}_y(\tau)=\mathbf{A}\mathbf{R}_s(\tau)\mathbf{A}^H$, We assume uncorrelated emissions, thus $\mathbf{R}_s(\tau)$ is diagonal. For $\tau=0$ we formulate the following convex optimization problem

$$\min_{\mathbf{x}\geq\mathbf{0}}\lambda||\mathbf{x}||_1+\frac{1}{2}\left|\left|\mathbf{R}_y(0)-\sum_{l=1}^{N^2}\mathbf{a}_l\mathbf{a}_l^Hx_l\right|\right|_F^2, \tag{3}$$

where $\lambda\geq 0$ is a regularization parameter and $\mathbf{x}=\text{diag}\{\mathbf{R}_s(0)\}$, the variance of each emitter. We solve (3) using a very efficient frequency domain implementation and the FISTA algorithm [7]. Pixel values in the final image correspond to the recovered variance of each emitter on the high-resolution grid. Similar construction is done for ultrasound scans to achieve super-resolution imaging of blood vessels.

III. Results and Conclusions

In this work, we improve the spatio-temporal resolution trade-off in fluorescence microscopy. Our work may facilitate real-time capturing of intra-cellular dynamics in microscopy, and fast sub-diffraction ultrasound blood-flow dynamics monitoring within living subjects.

Reconstruction results can be seen in Figs 1-3.

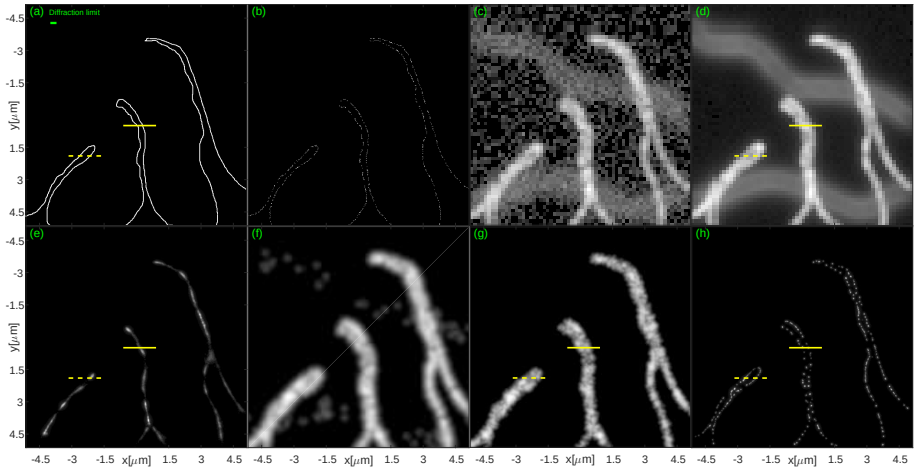

Fig. 1: **Reconstruction performance comparison of different methods of simulated sub-cellular microtubules. Upper row: unprocessed data.** (a) Ground truth: high resolution image of simulated sub-wavelength features (512×512 pixels). (b) Positions of emitters in the first frame of the movie. (c) Single diffraction limited frame from the movie (64×64 pixels), created by convolving the figure from (b) with the PSF [8] and adding Gaussian noise. The image includes unwanted background thick lines representing out-of-focus objects. (d) Diffraction-limited image, taken by averaging all the frames in the movie. **Lower row: recovered images** (e) ThunderSTORM [9] (f) Correlation SOFI (zero time-lag) [10]. (g) 4^{th} order SOFI (in absolute value, zero time-lag). (h) SPARCOM (512×512 pixels).

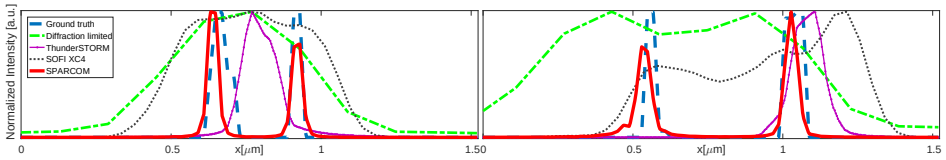

Fig. 2: Normalized cross-sections along the solid yellow line (left) and the dashed yellow line (right) of Fig. 1, comparing the ground truth (dashed blue, Fig. 1a), diffraction-limited image (dash dot green, Fig. 1d), ThunderSTORM (solid thin purple, Fig. 1e), 4^{th} order SOFI (black dot, Fig. 1g), and SPARCOM (solid red, Fig. 1h).

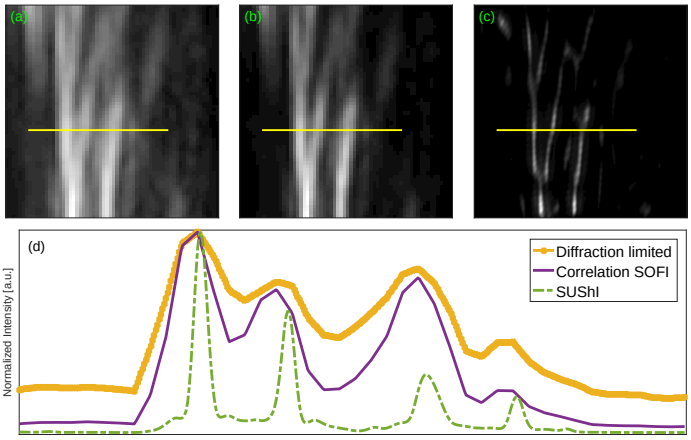

Fig. 3: **Reconstruction performance of CEUS of a blood vessel within the kidney of a New Zealand white rabbit.** (a) diffraction limited image, created by summing all frames (64×64 pixels). (b) Correlation SOFI reconstruction, zero time-lag. (c) SUSHI (512×512 pixels). (d) Intensity profiles along the yellow line. Diffraction limit in bold orange, correlation SOFI in solid purple and SUSHI in dash dot green.

REFERENCES

[1] E. Betzig, G. H. Patterson, R. Sougrat, O. W. Lindwasser, S. Olenych, J. S. Bonifacino, M. W. Davidson, J. Lippincott-Schwartz, and H. F. Hess, "Imaging intracellular fluorescent proteins at nanometer resolution." *Science (New York, N.Y.)*, vol. 313, no. 5793, pp. 1642–1645, 2006.

[2] M. J. Rust, M. Bates, and X. Zhuang, "Sub-diffraction-limit imaging by stochastic optical reconstruction microscopy (STORM)." *Nature methods*, vol. 3, no. 10, pp. 793–795, 2006.

[3] Y. Desailly, O. Couture, M. Fink, and M. Tanter, "Sono-activated ultrasound localization microscopy," *Applied Physics Letters*, vol. 103, no. 17, p. 174107, 2013.

[4] C. Errico, J. Pierre, S. Pezet, Y. Desailly, Z. Lenkei, O. Couture, and M. Tanter, "Ultrafast ultrasound localization microscopy for deep super-resolution vascular imaging," *Nature*, vol. 527, no. 7579, pp. 499–502, 2015. [Online]. Available: http://www.nature.com/doifinder/10.1038/nature16066

[5] T. Dertinger, R. Colyer, G. Iyer, S. Weiss, and J. Enderlein, "Fast, background-free, 3D super-resolution optical fluctuation imaging (SOFI)." *Proceedings of the National Academy of Sciences of the United States of America*, vol. 106, no. 52, pp. 22 287–22 292, 2009.

[6] A. Bar-Zion, C. Tremblay-Darveau, O. Solomon, D. Adam, and Y. Eldar, "Fast vascular ultrasound imaging with enhanced spatial resolution and background rejection," *IEEE Transactions on Medical Imaging*, 2016.

[7] A. Beck and M. Teboulle, "A Fast Iterative Shrinkage-Thresholding Algorithm," *SIAM Journal on Imaging Sciences*, vol. 2, no. 1, pp. 183–202, 2009.

[8] H. Kirshner, F. Aguet, D. Sage, and M. Unser, "3D PSF fitting for fluorescence microscopy: implementation and localization application," *Journal of microscopy*, vol. 249, no. 1, pp. 13–25, 2013.

[9] M. Ovesnỳ, P. Křížek, J. Borkovec, Z. Švindrych, and G. M. Hagen, "Thunderstorm: a comprehensive ImageJ plug-in for palm and storm data analysis and super-resolution imaging," *Bioinformatics*, vol. 30, no. 16, pp. 2389–2390, 2014.

[10] S. Geissbuehler, N. L. Bocchio, C. Dellagiacoma, C. Berclaz, M. Leutenegger, and T. Lasser, "Mapping molecular statistics with balanced super-resolution optical fluctuation imaging (bsofi)," *Optical Nanoscopy*, vol. 1, no. 1, p. 1, 2012.